Polylactosamine on glycoproteins influences basal levels of lymphocyte and macrophage activation

Akira Togayachi*, Yuko Kozono*, Hiroyasu Ishida*†, Sumie Abe*, Nami Suzuki*, Yuki Tsunoda*, Kozue Hagiwara*, Atsushi Kuno*, Takashi Ohkura*, Nobuo Sato*, Takashi Sato*, Jun Hirabayashi*, Yuzuru Ikehara*, Kouichi Tachibana*, and Hisashi Narimatsu*‡

*Research Center for Medical Glycoscience, National Institute of Advanced Industrial Science and Technology, Central-2 OSL, 1-1-1 Umezono, Tsukuba, Ibaraki 305-8568, Japan; and †Department of Gastroenterology, Institute of Clinical Medicine, University of Tsukuba, 1-1-1 Tenno-dai, Tsukuba, Ibaraki 305-8575, Japan

Communicated by Senitiroh Hakomori, Pacific Northwest Research Institute and University of Washington, Seattle, WA, August 9, 2007 (received for review April 13, 2007)

β1,3-*N*-acetylglucosaminyltransferase 2 (β3GnT2) is a polylactosamine synthase that synthesizes a backbone structure of carbohydrate structures onto glycoproteins. Here we generated β3GnT2-deficient (β3GnT2$^{-/-}$) mice and showed that polylactosamine on *N*-glycans was markedly reduced in their immunological tissues. In WT mice, polylactosamine was present on CD28 and CD19, both known immune costimulatory molecules. However, polylactosamine levels on these molecules were reduced in β3GnT2$^{-/-}$ mice. β3GnT2$^{-/-}$ T cells lacking polylactosamine were more sensitive to the induction of intracellular calcium flux on stimulation with anti-CD3ε/CD28 and proliferated more strongly than T cells from WT mice. β3GnT2$^{-/-}$ B cells also showed hyperproliferation on BCR stimulation. Macrophages from β3GnT2$^{-/-}$ mice had higher cell surface CD14 levels and enhanced responses to endotoxin. These results indicate that polylactosamine on *N*-glycans is a putative immune regulatory factor presumably suppressing excessive responses during immune reactions.

β-1,3-*N*-acetylglucosaminyltransferase | glycosyltransferase | hyperactivation | immune response

Carbohydrate structures participate in processes such as cell–cell, receptor–ligand, and carbohydrate–carbohydrate interactions (1). The biological functions of polylactosamine have been elucidated in several studies. Polylactosamine containing repeats of the *N*-acetyllactosamine (LacNAc) unit (Galβ1–4GlcNAcβ1–3)*n* is a fundamental structure of glycans carried on *N*- and *O*-glycans (2, 3) and glycolipid (4). Human blood group i and I antigens are linear and branched polylactosamine structures, respectively (5, 6).

Polylactosamines are further modified by the addition of different carbohydrate antigens such as Lewis and sialyl Lewis x (sLe^x) antigens. The latter is a selectin ligand consisting of a combination of sialyl and fucosyl residues with a polylactosamine structure (7, 8). It has been reported that the differential glycosylation of cell surface proteins regulates immunological processes, such as T cell activation, migration, and apoptosis (9), and that dramatic remodeling of *N*-glycans occurs on the surface of activated T cells. Such remodeling may affect the recognition of glycan structures by lectins such as selectins, siglecs, and galectins, and thereby alter biological functions (10).

The length of the polylactosamine chain is an important factor in immune responses. Polylactosamine inhibits NK cell-mediated cytotoxicity by its effects on the cell-binding process (11). Thus, NK cells recognize cancer target cells that possess sLe^x antigens on *N*-glycans with rather short polylactosamine chains (12). *N*-acetylglucosaminyltransferase 5 (MGAT5) is a glycosyltransferase that synthesizes β1,6 branching of *N*-glycan candidate structures for polylactosamine (13). T cells of Mgat5$^{-/-}$ mice have increased sensitivity to activation due to lack of surface interactions between the TCR complex and the endogenous polylactosamine-binding lectin, galectin-3 (14).

Polylactosamine carried on *N*- and *O*-glycans is coordinately synthesized by the alternative action of a β1,4-galactosyltransferase and a β1,3-*N*-acetylglucosaminyltransferase (β3GnT). Eight β3GnTs, β3GnT1 to β3GnT8, have been isolated, and their *in vitro* enzymatic activities have been characterized (15). However, the roles of these multiple β3GnTs in *in vivo* polylactosamine synthesis are still unclear. Because β3GnT2 possesses strong polylactosamine synthesizing activity on oligosaccharide substrates *in vitro*, it is a good candidate for acting as a polylactosamine synthase *in vivo* (16, 17). Thus, we predicted that long polylactosamine chains on glycoproteins would be lost or shorter in β3GnT2-deficient (β3GnT2$^{-/-}$) mice, and immune cells lacking polylactosamine would have altered immune responses. Here we show that polylactosamine on *N*-glycans is markedly reduced in immunological tissues in β3GnT2$^{-/-}$ mice, and their immune cells are hyperreactive.

Results

***N*-Glycan Polylactosamine Is Markedly Reduced in β3GnT2$^{-/-}$ Mice.** Because *β3GnT2* transcripts were expressed in lymphocytes and macrophages of adult WT mice [supporting information (SI) Fig. 5], we generated β3GnT2$^{-/-}$ mice to analyze immunological phenotypes in the absence of this gene. First, we examined glycan structures in tissues of β3GnT2$^{-/-}$ mice. Carbohydrate structures potentially generated by β3GnT2 are schematically shown in Fig. 1*A* based on the *in vitro* substrate specificity of β3GnT2. To investigate potential alterations of polylactosamine on glycoproteins in β3GnT2$^{-/-}$ mice, we performed lectin blot analysis with the *Lycopersicon esculentum* (tomato) lectin (LEL), which is known to bind to polylactosamines with at least three lactosamine unit repeats (18, 19). Intense smeared bands were observed in LEL blots of thymus, spleen, or macrophages of WT and β3GnT2$^{-/+}$ mice, indicating the expression of many glycoproteins bearing polylactosamine in these tissues/cells (Fig. 1*B*). In contrast, the intensity of LEL bands in β3GnT2$^{-/-}$ mice was dramatically reduced in all three cell types. These results indicate that the LEL-detectable polylactosamine on glycoproteins was synthesized mostly by β3GnT2 in these tissues. After *N*-glycan digestion with *N*-glycanase F (PNGase F), the LEL-positive bands disappeared almost completely. This result strongly sug-

Author contributions: A.T. and Y.K. contributed equally to this work; A.T., Y.K., H.I., A.K., T.S., Y.I., K.T., and H.N. designed research; A.T., Y.K., H.I., S.A., N. Suzuki, Y.T., K.H., A.K., T.O., and N. Sato performed research; A.K. and J.H. contributed new reagents/analytic tools; A.T., Y.K., H.I., S.A., N. Suzuki, Y.T., K.H., A.K., T.O., N. Sato, T.S., Y.I., K.T., and H.N. analyzed data; and A.T., K.T., and H.N. wrote the paper.

The authors declare no conflict of interest.

Abbreviations: LEL, *Lycopersicon esculentum* (tomato) lectin; DSA, *Datura stramonium* agglutinin; MFI, mean fluorescence intensity.

‡To whom correspondence should be addressed. E-mail: h.narimatsu@aist.go.jp.

This article contains supporting information online at www.pnas.org/cgi/content/full/0707426104/DC1.

IMMUNOLOGY

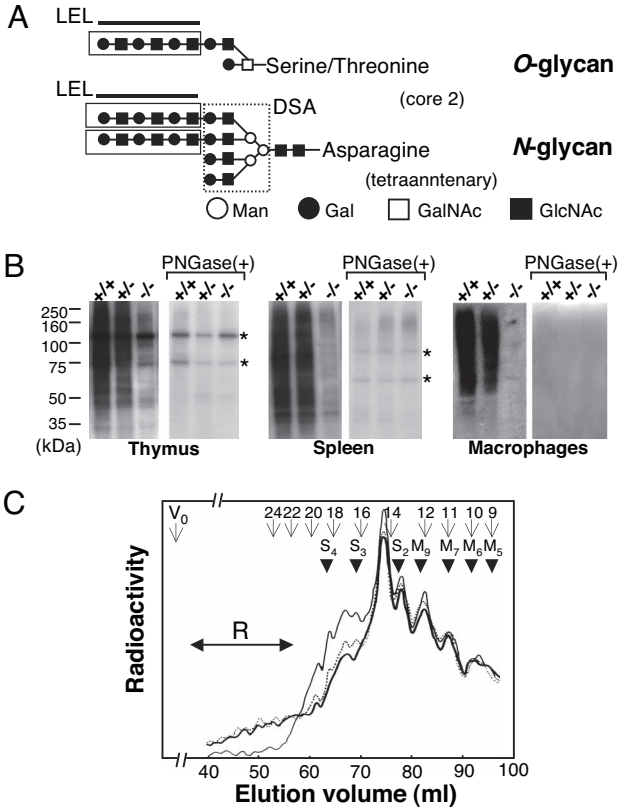

Fig. 1. Decreased numbers of polylactosamine repeating units on *N*-glycan oligosaccharides in β3GnT2$^{-/-}$ mice. (*A*) Predicted carbohydrate structures possibly absent in β3GnT2$^{-/-}$ mice are indicated by rectangles. The bar indicates the LEL-binding epitope consisting of more than three repeated lactosamine units. The dotted rectangle indicates the DSA-binding structure that represents tri- and tetraantenna *N*-glycans. (*B*) Lysates of thymus, spleen, and macrophages were incubated in the absence or presence of *N*-glycanase F (PNGase F) overnight and subjected to LEL blots for polylactosamine. +/+, WT; +/−, heterozygous; −/−, homozygous null. The asterisks indicate nonspecific bands recognized by HRP-streptavidin. The positions of molecular mass markers are indicated. (*C*) Bio-Gel P-4 column chromatography of desialylated *N*-glycans derived from stimulated T cells of WT (bold line), β3GnT2$^{+/-}$ (dotted line), and β3GnT2$^{-/-}$ mice (solid line). Arrows with the numbers 9–24 indicate the elution positions of glucose oligomers, and the numbers indicate glucose units. Arrows with M_{5-9} and S_{2-4} indicate the elution positions of standard oligosaccharides, Man_{5-9}·GlcNAc·$GlcNAc_{OT}$ and $(Gal{\cdot}GlcNAc)_{2-4}$·Man_3·GlcNAc·$GlcNAc_{OT}$, respectively. Arrows with R indicate the elution range of oligosaccharides bearing putative polylactosamine repeating units.

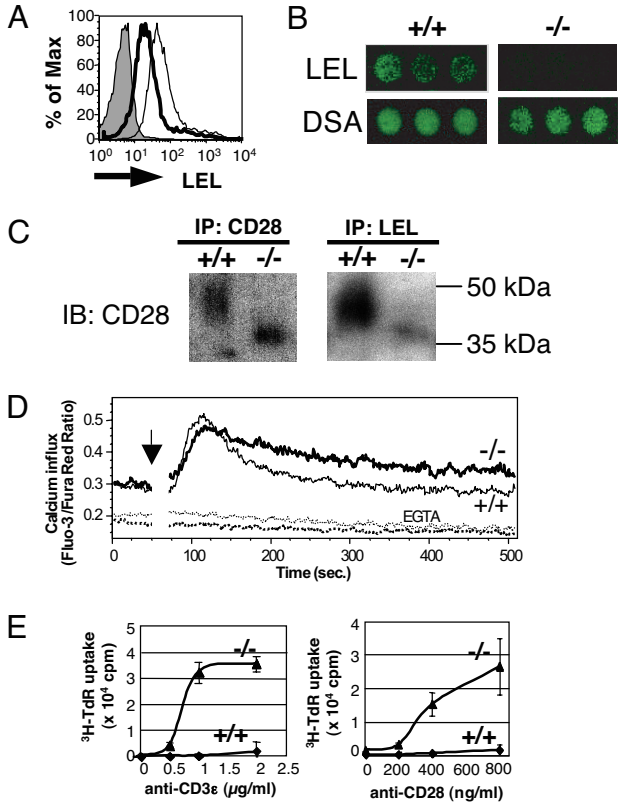

Fig. 2. T cells from β3GnT2$^{-/-}$ mice are hypersensitive to stimulation by TCR/CD28. (*A*) Isolated splenic T cells stained with FITC-LEL. The shaded peak indicates the no lectin control. Mean fluorescence intensity (MFI) on LEL staining was 32 for WT (solid line) and 11 for β3GnT2$^{-/-}$ (bold line) cells. (*B*) Glycan analysis of immunoprecipitated CD28 protein by lectin microarraying. The signals of LEL (reactive to polylactosamine) and DSA (reactive to tri- and tetraantennary *N*-glycan structures) are shown. (*C*) CD28 proteins detected on Western blot with anti-mouse CD28 (M-20; Santa Cruz Biotechnology, Santa Cruz, CA). Immunoprecipitation with anti-CD28 mAb (*Left*) or LEL-agarose (*Right*). The same volume of each extract from WT and β3GnT2$^{-/-}$ splenic T cells was subjected to Western blot analysis. (*D*) The calcium response was induced by anti-CD3ε/anti-CD28 antibodies. Splenic T cells were loaded with Fluo-3 and Fura-Red dyes. Arrows indicate the time of addition of streptavidin for cross-linking of receptors. (*E*) Splenic T cells cultured with the indicated doses of immobilized anti-CD3ε and 750 ng/ml of soluble anti-CD28 antibodies (*Left*), or reciprocally with immobilized CD3ε (1 μg/ml) and the indicated doses of soluble anti-CD28 antibodies (*Right*). Proliferative responses are given as [^{3}H]TdR incorporation for the final 6 h of the 42 h culture period. Each assay was performed in triplicate, and all data are representative of three to five experiments.

gests that polylactosamine with more than three repeating units is mainly present on *N*-glycans.

To investigate the *N*-glycan structures in T cells of WT and β3GnT2$^{-/-}$ mice, splenic T cells were stimulated with anti-CD3ε and anti-CD28 and metabolically labeled with [^{3}H]glucosamine. *N*-glycans isolated from these labeled cells were then analyzed by Bio-Gel P-4 gel permeation chromatography. In Fig. 1*C*, standard tri- and tetraanntenary *N*-glycan without polylactosamine was fractionated at S_3 and S_4, respectively, while *N*-glycans with higher molecular weights than standard *N*-glycan appeared in the range indicated as R. In β3GnT2$^{-/-}$ mice, *N*-glycans fractionated as R were markedly reduced, whereas those at S_3 and S_4 were relatively increased. We obtained similar results with splenocytes (data not shown). The higher molecular weight fractions indicated as R contain *N*-glycans with polylactosamine, whereas S_3 and S_4 fractions represent tri- and tetraanntenary *N*-glycan without polylactosamine. This finding suggests that polylactosamine on *N*-glycan was reduced in β3GnT2$^{-/-}$ T cells.

Polylactosamine on *N*-Glycan of CD28 Molecules Is Diminished, and T Cells in β3GnT2$^{-/-}$ Mice Are Hypersensitive to TCR/CD28 Stimulation. To investigate potential alterations in immune cell development in β3GnT2$^{-/-}$ mice, we analyzed the expression of cell surface CD antigens by flow cytometry. No obvious differences were observed in B and T cell subpopulations in splenocytes or thymocytes from β3GnT2$^{-/-}$ or WT mice as shown in SI Fig. 6 *A* and *B*. Thus, β3GnT2 deficiency appeared to have no marked effect on T and B cell development. However, both splenic T cells (Fig. 2*A*) and thymocytes (SI Fig. 6*C*) from β3GnT2$^{-/-}$ mice stained with LEL at reduced intensity. To identify a T cell surface molecule carrying polylactosamine, we screened molecules such as CD4, CD8α, and CD28 from WT mice by lectin microarray analysis and found that the LEL signal was decreased on immunoprecipitated CD28 in β3GnT2$^{-/-}$ compared with WT mice (Fig. 2*B*). No clear difference in CD28 *Datura stramonium* agglutinin (DSA) signals, which represent tri- and

tetraantennary *N*-glycan structures, was observed. These results suggest that the decrease of polylactosamine on CD28 in β3GnT2$^{-/-}$ T cells occurs despite the presence of *N*-glycan core structures. No LEL signal was observed on CD4 and CD8α molecules in WT or β3GnT2$^{-/-}$ mice (data not shown).

By Western blotting with anti-CD28 antibody, we showed that the CD28 molecules from β3GnT2$^{-/-}$ splenic T cells migrated faster in SDS/PAGE than WT (Fig. 2*C*). This mobility shift of CD28 also was observed in β3GnT2$^{-/-}$ thymocytes (data not shown). These results are consistent with a reduction of CD28 molecular weight due to decreased polylactosamine. In β3GnT2$^{-/-}$ mice, the CD28 molecule in LEL-agarose immunoprecipitates was barely detectable, but the same reduction of its molecular weight also was observed. Because murine CD28 has four potential *N*-glycosylation sites, it is conceivable that the mobility shift of CD28 observed in β3GnT2$^{-/-}$ T cells is due to the decrease of polylactosamine on *N*-glycans.

Because the biological function of polylactosamine on T cell surface proteins including CD28 had not been addressed, we investigated functional differences between WT and β3GnT2$^{-/-}$ T cells. First, we performed intracellular calcium assays to compare the response of WT and β3GnT2$^{-/-}$ T cells to anti-CD3/anti-CD28 stimulation. As shown in Fig. 2*D*, the initial transient peak of intracellular calcium concentration within a few minutes of TCR and CD28 cross-linking was essentially identical in WT and β3GnT2$^{-/-}$ splenic T cells. Thereafter, it decreased more slowly to the basal level in β3GnT2$^{-/-}$ than in WT splenic T cells. This finding suggests that decreased polylactosamine results in maintenance of prolonged intracellular calcium concentrations after CD3/CD28 stimulation.

Next, we investigated CD3/CD28-induced T cell proliferation. In β3GnT2$^{-/-}$ splenic T cells, [^{3}H]-thymidine uptake was already measurable at day 2 in an anti-CD3ε and anti-CD28 dose-dependent manner, but not in WT T cells (Fig. 2*E*), which proliferated later (data not shown). Thus, the polylactosamine deficiency of cell surface receptors such as CD28 can accelerate their downstream signaling and T cell proliferation.

Polylactosamine on CD19 Molecules Is Diminished in Splenic B Cells of β3GnT2$^{-/-}$ Mice. Splenic B cells from β3GnT2$^{-/-}$ mice also showed significant decreases in LEL staining (Fig. 3*A*). To determine which structures carried polylactosamine, we screened B cell surface molecules such as BCR, CD19, and CD21/35 using lectin microarrays. It was found that the LEL signal was decreased on immunoprecipitated CD19 (Fig. 3*B*). Weak LEL signals were detected on WT BCR and CD21/35; these signals may have been decreased in β3GnT2$^{-/-}$ mice (data not shown). No obvious difference in CD19 DSA signals between WT and β3GnT2$^{-/-}$ mice was observed. Western blotting confirmed that polylactosamine is carried on CD19. Fig. 3*C* shows that CD19 from β3GnT2$^{-/-}$ splenic B cells migrated faster than WT in SDS/PAGE. In addition, the CD19 molecule was only marginally detected in LEL-agarose immunoprecipitates from β3GnT2$^{-/-}$ mice (Fig. 3*C Right*). These results suggest that polylactosamine is carried on CD19 molecules. Because CD19 is a costimulatory molecule in B cell activation (20), we examined the effect of polylactosamine deficiency on B cell proliferation. Resting B cells were stimulated with anti-IgM, and proliferation was assessed after 2 days. Greater proliferation of β3GnT2$^{-/-}$ than WT splenic B cells was observed with low concentrations of anti-IgM (Fig. 3*D*). These results suggest that decreased polylactosamine in B cells lowers the cellular threshold for proliferation triggered by BCR stimulation.

F4/80$^+$ Peritoneal Macrophages from β3GnT2$^{-/-}$ Mice Are Hypersensitive to LPS Stimulation. Because β3GnT2$^{-/-}$ T and B cells showed hypersensitivity to immune stimulation, we also investigated other immune responses in β3GnT2$^{-/-}$ macrophages,

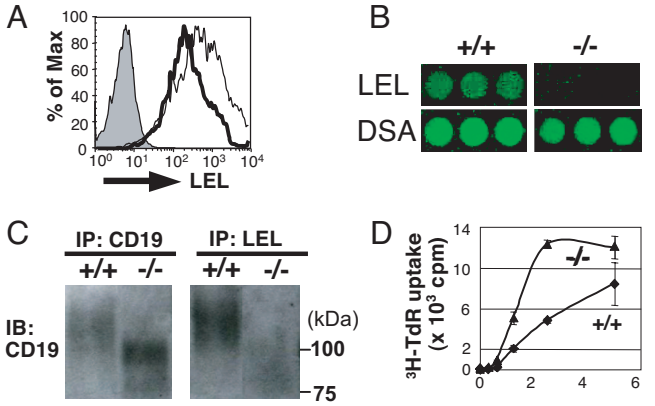

Fig. 3. Resting B cells from β3GnT2$^{-/-}$ mice are hypersensitive to BCR-mediated stimulation. (*A*) Isolated B cells stained with FITC-LEL. The shaded peak indicates the no lectin control. MFI on LEL staining was 1,267 for WT (solid line) and 717 for β3GnT2$^{-/-}$ (bold line) cells. (*B*) Glycan analysis of immunoprecipitated CD19 protein by lectin microarraying. The signals of LEL (reactive to polylactosamine) and DSA (reactive to tri- and tetraantenna *N*-glycan structures) are shown. (*C*) CD19 proteins detected on Western blot with anti-mouse CD19 (Cell Signaling Technology). Immunoprecipitation with anti-CD19 antibody or LEL agarose. The same volume of each extract was subjected to Western blot. (*D*) Resting B cells (ρ = 1.079) cultured with the indicated dose of F(ab')$_2$ anti-IgM. Proliferative responses are given as [^{3}H]TdR incorporation for the final 6 h of the 42 h culture period. Each assay was performed in triplicate, and all data are representative of two to four experiments.

especially LPS responsiveness. Peritoneal macrophages of WT mice were strongly stained with FITC-LEL, but staining intensity was significantly reduced in β3GnT2$^{-/-}$ cells (Fig. 4*A*). Next, we measured the production of inflammatory cytokines on LPS stimulation. β3GnT2$^{-/-}$ macrophages were found to produce more TNF-α, IL-1β, and IL-6 than WT macrophages (Fig. 4*B*). To further investigate the hyperresponsiveness to LPS in β3GnT2$^{-/-}$ macrophages, we analyzed the expression level of macrophage surface antigens by flow cytometry. CD14 expression was significantly up-regulated on the surface of β3GnT2$^{-/-}$ peritoneal macrophages (F4/80$^+$ peritoneal exudate cells) (Fig. 4*C*), but no other surface antigens including TLR4 were affected (data not shown). Western blotting showed that CD14 expression in β3GnT2$^{-/-}$ macrophages was up-regulated even in the absence of LPS (Fig. 4*D*), but stimulation with LPS resulted in a further increase.

Because LPS binding to CD14 on macrophages induces downstream signals, we investigated phosphorylated forms of ERK and p38, which were found to be present in significantly greater amounts in β3GnT2$^{-/-}$ cells. In contrast, the total amounts of ERK and p38 were similar in macrophages from WT and β3GnT2$^{-/-}$ mice (Fig. 4*E*). These results further underline the hyperresponsiveness of β3GnT2$^{-/-}$ macrophages to LPS, suggesting the involvement of polylactosamine in the immune response of macrophages.

Discussion

Here we show that LEL-detectable polylactosamine on *N*-glycans is markedly decreased in β3GnT2$^{-/-}$ mice, suggesting that β3GnT2 is the major enzyme responsible for the synthesis of polylactosamine on *N*-glycans *in vivo*. We explored cell surface molecules that lost polylactosamine in β3GnT2$^{-/-}$ mouse-derived cells. Furthermore, we identified functionally relevant reductions of polylactosamine on the costimulatory molecules CD28 and CD19. Thus, the T and B cells of β3GnT2$^{-/-}$ mice proliferated more strongly to TCR or BCR stimulation than WT

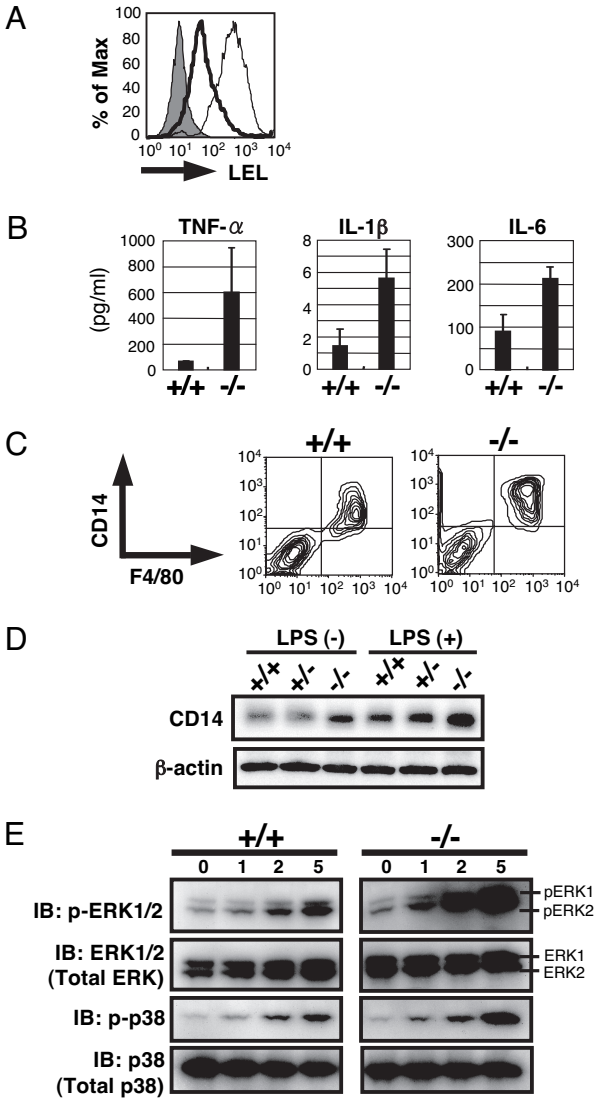

Fig. 4. Peritoneal macrophages from β3GnT2$^{-/-}$ mice are hypersensitive to LPS stimulation. (*A*) Peritoneal macrophages stained with LEL. The shaded peak indicates the no lectin control. MFI on LEL staining was 767 for WT (solid line) and 188 for β3GnT2$^{-/-}$ (bold line) cells. (*B*) Peritoneal macrophages stimulated with LPS for 6 h. Cytokine production measured by ELISA. Data are given as means and standard deviation of triplicate determinations. Stimulated β3GnT2$^{-/-}$ macrophages produced significantly greater amounts of cytokine than WT (TNF-α, $P = 0.037$; IL-1β, $P = 0.0077$; IL-6, $P = 0.0048$). (*C*) Peritoneal cells stained with FITC-F4/80 and PE-CD14. CD14 expression was elevated ≈3-fold (MFI, 679) compared with WT mice (MFI, 216). (*D*) Peritoneal macrophages stimulated with LPS for 6 h. CD14 proteins detected on Western blot with anti-mouse CD14. (*E*) Peritoneal macrophages stimulated with LPS for the indicated time. Phosphorylation of ERK and p38 analyzed by immunoblots.

in vitro. In addition, we observed that β3GnT2$^{-/-}$ macrophages were hypersensitive to endotoxin.

In LEL lectin blot analysis, the high-intensity LEL-reactive bands from tissues of WT mice were completely absent from β3GnT2$^{-/-}$ mice and were not detected after PNGase F treatment. The binding specificity of LEL to long polylactosamine and the catalytic specificity of β3GnT2 in polylactosamine synthesis suggest that the LEL-detectable smeared bands from WT cells are mostly lactosamines on *N*-glycan. These results demonstrate that β3GnT2 is an essential enzyme for the biosynthesis of polylactosamine on *N*-glycans. It is still unclear whether β3GnT2 synthesizes polylactosamine on *O*-glycans as well because this finding may not be detectable by LEL blotting. No obvious difference between WT and β3GnT2$^{-/-}$ was observed on lectin blotting with PHA-L_4 or Con A, both recognizing *N*-glycan core structures (data not shown). These results can be interpreted to imply that the polylactosamine on *N*-glycans, but not their core structure, is altered by β3GnT2 deficiency. It has been conjectured that polylactosamine is preferentially present on the β1–6 branch of tetraantennary *N*-glycans (21, 22). It is known that a polylactosamine on glycolipids is present in erythrocytes (4, 23). We did not analyze glycolipids in the β3GnT2$^{-/-}$ mouse. However, we previously documented that only β3GnT5 can synthesize Lc_3Cer and nLc_5Cer, resulting in neolacto-series glycolipids, which contain polylactosamines (17). β3GnT5 is responsible for the synthesis of Lc_3Cer in hematopoietic cells (17, 24). We therefore assume that the expression of polylactosamines on neolacto-series glycolipids would not be affected in β3GnT2$^{-/-}$ mice. Taken together the data presented here suggest that the LEL-detectable long polylactosamine is synthesized by β3GnT2 on the β1–6 branches of *N*-glycans in WT mice and that long polylactosamine on tri- or tetraanntenary *N*-glycan is reduced in β3GnT2$^{-/-}$ mice.

We tried to identify cell surface proteins carrying polylactosamine and found that polylactosamines were detectable with LEL on CD28 and CD19 from WT T cells and B cells, respectively. However, they were only marginally detectable on β3GnT2$^{-/-}$ cells. Mobilities of CD28 and CD19 in SDS/PAGE were different in WT and β3GnT2$^{-/-}$ cells. Thus, we conclude that CD28 and CD19 molecules carry LEL-detectable polylactosamine and that β3GnT2 is involved in its synthesis. Both CD28 and CD19 have potential *N*-glycosylation sites (four and six, respectively) and migrate more slowly in SDS/PAGE than would be anticipated from their molecular weights.

CD28, a T cell surface molecule that interacts with B7 family proteins, is a major T cell costimulator (25). Therefore, glycosylation on CD28 can be involved in the regulation of CD28-mediated signaling. It has been reported that the *N*-glycan on CD28 molecules negatively regulates this T cell costimulation (26). Hypoglycosylation of *N*-glycan on CD28 regulates the binding affinity between the receptor and its ligand, as well as receptor clustering. Because we have shown that the polylactosamine carried on CD28 is on *N*-glycans, it is conceivable that it is involved in the negative regulation of CD28 signaling by modulating the interaction between receptor and ligand or receptor clustering. T cell hypersensitivity to stimulation in β3GnT2$^{-/-}$ mice is similar to the reported phenotype of MGAT5$^{-/-}$ mice (14). In the absence of MGAT5, clustering of the TCR was enhanced upon anti-CD3 antibody cross-linking. MGAT5 is a glycosyltransferase responsible for β1,6 branching of *N*-glycans to form tri- and tetraantennary *N*-glycans, to which polylactosamine are added (13). It is conceivable that functional polylactosamine, synthesized by β3GnT2 on WT T cells, extends β1,6 branching of tri- or tetraanntenary *N*-glycans synthesized by MGAT5. If this phenomenon is because of the loss of polylactosamine on the *N*-glycan, there will be some shared phenotype between β3GnT2$^{-/-}$ mice and MGAT5$^{-/-}$ mice. However, it is not known which glycoprotein is responsible for augmented T cell activation as a result of impaired *N*-glycan in MGAT5$^{-/-}$ mice. Although TCR and CD3 are thought to carry *N*-glycans, these molecules were only marginally detectable with LEL in our hands (data not shown). In contrast, CD28 is one of the major proteins carrying LEL-detectable carbohydrate. Because stimulation by both TCR/CD3 and CD28 is essential for T cell proliferation, the polylactosamine on CD28 may play a major role in regulating T cell activation. Like CD28 in T cells, CD19 is a B cell costimulatory molecule (20). B cells from CD19$^{-/-}$ mice showed impaired activation upon BCR stimulation (27). Because no direct association between BCR and CD19 has been

reported, the molecular mechanism whereby polylactosamine deficiency on CD19 leads to B cell hypersensitivity is unclear. However, because CD19 is at least one of the major B cell surface glycoproteins carrying polylactosamine, CD19 must be involved in the regulation of BCR-mediated B cell activation by an unknown mechanism. However, it has been reported that CD45 expressed on T and B cells is a major protein that reacts with anti-i and anti-I antibodies (28, 29) and contains mainly bi-, tri-, and tetraantennary complex-type sugar chains. Tetraantennary complex-type *N*-glycan (30) and *O*-glycan (28, 31) on CD45 possess polylactosamine. We investigated the glycans on CD45 molecules by lectin microarray analysis (data not shown) and found LEL signals on anti-CD45 mAb immunoprecipitates from WT leukocytes. LEL signals of such immunoprecipitates from β3GnT2$^{-/-}$ leukocytes were slightly decreased compared with those of WT leukocytes. In contrast, the polylactosamines on CD28 and CD19 in the β3GnT2$^{-/-}$ mouse were almost completely absent. No significant difference on the migration shift of CD45 molecules in SDS/PAGE was observed between WT and β3GnT2$^{-/-}$ mice, whereas mobilities of CD28 and CD19 were quite different. We examined the residual LEL-detectable polylactosamines in cell lysates after depletion of CD28 molecules (SI Fig. 7) or CD19 molecules (SI Fig. 8). Many LEL-reactive bands still remained after removal of the CD28 and the CD19 from the cell lysates. These findings suggest that many proteins, in addition to CD28 and CD19, carry LEL-detectable polylactosamine chains. Nevertheless, it is noteworthy that polylactosamine existed on both CD28 and CD19, which are known as costimulatory accessory molecules regulating signals in T and B cells, respectively. We posit that phenotypes in β3GnT2$^{-/-}$ lymphocytes are more likely to result from the loss of polylactosamine on CD28 and CD19 than CD45.

There are at least two possible molecular mechanisms responsible for immune regulation by polylactosamine. One is the inhibitory mass effect of polylactosamine on molecular interactions. It was reported that the numbers and sizes of *N*-glycans attached to various cell surface receptors, such as TCR/CD3, pMHC, CD4, and CD8, regulate the clustering and association of these receptor proteins (32, 33). Because the size of a typical *N*-glycan is comparable to an Ig domain, it is conceivable that the abundance and size of *N*-glycans, especially those with polylactosamine, play important roles in controlling the assembly and stabilization of the receptor complexes. To test this hypothesis, we need to further elucidate which molecular interaction is augmented by polylactosamine deficiency. Another possibility is glycan-mediated molecular interactions. sLe^x antigens and sialic acids on polylactosamine are known ligands for selectin and siglecs, respectively (34, 35). Polylactosamine might be a ligand for cellular lectins such as galectins (36, 37). To support the latter hypothesis, however, it would be essential to identify specific lectins for polylactosamine or carbohydrate ligands.

CD14 overexpression increases reactivity to LPS (38). We also observed that macrophages from β3GnT2$^{-/-}$ mice expressed higher levels of CD14 and were hyperresponsive to LPS stimulation for that reason. Because polylactosamine was not detected on macrophage LPS receptors, including CD14, by lectin microarrays, it is unlikely that the LPS hyperresponsiveness of β3GnT2$^{-/-}$ macrophages is due to modulation of receptor interaction. We observed up-regulated expression of CD14 mRNA in β3GnT2$^{-/-}$ macrophages (data not shown). Because LPS stimulation augments CD14 expression, macrophages from β3GnT2$^{-/-}$ mice may already be in an activated state. A potential reason for the augmented CD14 expression and/or *in vivo* activation of β3GnT2$^{-/-}$ macrophage is either polylactosamine deficiency of some other macrophage surface molecules or possibly activation after interactions with polylactosamine-deficient T and/or B cells. Because T and B cells from β3GnT2$^{-/-}$ mice were hypersensitive to stimulation at least *in vitro*, they may have activated macrophages *in vivo*.

In summary, our study documents deficiency of LEL-detectable polylactosamine on *N*-glycans and *in vitro* hyperresponsiveness of T cells, B cells, and macrophages from β3GnT2$^{-/-}$ mice. Polylactosamine deficiency appears to be involved in the immunological disorders observed in these mice. Therefore, this study suggests that polylactosamine on *N*-glycans suppresses excessive immune responses and regulates basal levels of immune reactivity. Although we have not determined the molecular basis of the regulatory mechanism of polylactosamine in immune responses yet, we did identify it on two important costimulatory molecules, CD28 and CD19. We anticipate that these studies will lead to a better understanding of the regulatory mechanisms of immune responses and the biological functions of polylactosamine.

Materials and Methods

Generation of β3GnT2$^{-/-}$ Mice. To investigate the function of β3GnT2 and polylactosamine, we obtained β3GnT2$^{-/-}$ mice by using Omnibank (Lexicon Genetics, The Woodlands, TX) (39). β3GnT2$^{-/-}$ mice were generated by using a random mutagenesis method based on gene trapping with the retroviral vector, VICTR20 (39). The β3GnT2$^{-/-}$ mice were backcrossed onto a C57BL/6N (Charles River Japan, Yokohama, Japan) background. Detailed information on the β3GnT2$^{-/-}$ mice, including PCR conditions for genotyping and mouse handling, is given in SI Fig. 5.

Lectin-Blot Analysis with LEL. Cells were solubilized by brief sonication with 20 mM Hepes buffer (pH 7.2) containing 2% Triton X-100, 150 mM $NaCl_2$, and complete protease inhibitor mixture (Roche Diagnostics, Basel, Switzerland). *N*-glycan oligosaccharides were digested by *N*-glycopeptidase F (Takara, Kyoto, Japan). Ten micrograms of homogenized proteins were separated by 10% SDS/PAGE, transferred to membranes, and blotted with biotinylated LEL (Vector Laboratories, Burlingame, CA)/streptavidin-HRP (Amersham Biosciences, Piscataway, NJ).

Metabolic Labeling of Costimulated T Cells. Isolated T cells (2×10^6/ml) were cultured with immobilized anti-CD3ε (1 μg/ml) and 750 ng/ml of anti-CD28 in multiple wells of 24-well plates for 66 h. Supernatants were then replaced with RPMI medium 1640 substituting one fifth of the glucose with [^{3}H]glucosamine (1 MBq/ml) and 5% FBS. The cells were homogenized and then completely dried before hydrazinolysis as previously described (40). After *N*-acetylation and *Arthrobacter* sialidase (Nacalai Tesque, Kyoto, Japan) digestion, oligosaccharides were analyzed by Bio-Gel P-4 column chromatography as previously described (41). Radioactivity was determined with an Aloka LSC-6101 liquid scintillation spectrometer.

Flow Cytometry. Cells were stained in 1% BSA, 0.1% NaN_3-PBS containing antibodies as follows: CD19 (1D3), CD3ε (145-2C11), CD4 (RM4-5), CD8α (53-6.7), CD14 (Sa2-8), CD11a (2D7), CD11b (M1/70), CD11c (HL3), CD45 (Ly-5: 30-F11), CD45R/B220 (RA3-6B2), CD62L (MEL-14), TER-119 (Ly-76: TER-119), Gr-1 (Ly-6C/G: RB6-8C5), F4/80 (BM8), isotype control Ig, or FITC-LEL (purchased from BD Biosciences PharMingen, San Diego, CA; eBioscience, San Diego, CA; BioLegend, San Diego, CA; or Vector Laboratories, Burlingame, CA). Data were acquired using a FACSCalibur (Becton Dickinson, San Jose, CA).

Immunoprecipitation and Lectin Microarray. Cell surface immunoprecipitated proteins were analyzed by using lectin microarrays. For this purpose, surface proteins of isolated T or B cells were labeled with sulfo-NHS-LC-biotin (Pierce Chemical , Rockford, IL) and lysates immunoprecipitated. Lectin microarrays were

performed following Kuno *et al.* (42). To visualize the glycans native to cell surface proteins, interactions of the biotinylated target protein with the lectins immobilized on glass slides were detected by the Cy3-streptavidin method. Briefly, immunoprecipitated protein was released and then applied to the lectin array containing triplicate spots of 43 lectins (42). The glass slide was scanned by an evanescent-field fluorescence scanner, SC-Profiler (Moritex, Yokohama, Japan).

Calcium Flux Analysis. Intracellular calcium was analyzed by the ratiometric Fluo-3/Fura Red combination method (43). Cells were loaded with 4 μg/ml Fluo-3-AM and 10 μg/ml Fura-Red-AM (Invitrogen, Carlsbad, CA) in the presence of pluronic F127 detergent (Invitrogen; final concentration 0.02%) and 1 mM probenecid for 30 min at 37°C. The biotinylated anti-CD3ε and anti-CD28 were incubated for 15 min on ice. Cells were warmed to 37°C for 10 min before use. Calcium flux was measured by using a FACSCalibur flow cytometer. After 55 sec measuring baseline calcium level, streptavidin was added to cross-link antibodies. The mean ratio of Fluo-3/Fura Red fluorescence was measured during the acquisition time course and expressed graphically by FlowJo software (Tree Star, Ashland, OR).

T and B Cell Isolation and Proliferation Assays. T cells were isolated with a MACS Pan T cell Isolation kit (Miltenyi Biotec, Auburn, CA). T cells (2×10^6/ml) were stimulated with immobilized anti-CD3ε (145–2C11) and soluble anti-CD28 (37.51) antibodies in RPMI-1640 culture medium in 96-well flat-bottomed plates for 42–86 h. Resting B cells ($\rho = 1.079$) were isolated by a MACS B cell isolation kit (Miltenyi Biotec) followed by discontinuous Percoll (Amersham Pharmacia) gradient centrifugation. Resting B cells (2×10^6/ml) were cultured with goat $F(ab')_2$ anti-IgM (Southern Biotechnology Associates, Birmingham, AL) for 42 h. Cultures in triplicate were pulsed for the final 6–8 h with [^{3}H]thymidine (0.25 μCi/well) and harvested by using a 96-well plate harvester. The incorporated radioactivity was measured by using a microplate beta 1450 counter (Wallac, Gaithersburg, MD).

Peritoneal Macrophage Isolation and Stimulation. Thioglycolate-induced peritoneal exudate cells were plated to allow macrophages to adhere to the culture dish. For signaling assays, 1×10^6 cells were stimulated with 100 ng/ml of LPS derived from 50 μl *Escherichia coli* 0111:B4 (Sigma–Aldrich, St. Louis, MO). Antibodies used for Western blots were rabbit anti-ERK, anti-phospho-ERK, anti-p38, anti-phospho-p38 (Cell Signaling Technology, Danvers, MA), anti-CD14 (rmC5-3; BD Biosciences PharMingen), and anti-β-actin (Sigma–Aldrich). For cytokine assays, 1×10^6 cells/ml were cultured in the absence or presence of 100 ng/ml LPS in a 24-well plate for 6 h. Cytokines in the supernatants were measured by ELISA (eBioSciences and Endogen, Woburn, MA).

We thank Drs. Takashi Angata, Akihiko Kameyama, Hiromi Ito, and Hideki Matsuzaki, Mr. Noboru Uchiyama, and Ms. Mihou Fushimi (National Institute of Advanced Industrial Science and Technology, Tsukuba, Japan) for helpful advice and excellent assistance; Drs. Takashi Kudo and Satoru Takahashi (Tsukuba University, Japan) for helpful advice; and Drs. Noriko Tsuji (National Institute of Advanced Industrial Science and Technology, Tsukuba, Japan) and Takashi Saito (RIKEN, Saitama, Japan) for the kind gift of antibodies. This work was supported by the New Energy and Industrial Technology Development Organization.

1. Varki A (1993) *Glycobiology* 3:97–130.
2. Fukuda M, Bothner B, Ramsamooj P, Dell A, Tiller PR, Varki A, Klock JC (1985) *J Biol Chem* 260:12957–12967.
3. Fukuda M, Carlsson SR, Klock JC, Dell A (1986) *J Biol Chem* 261:12796–12806.
4. Watanabe K, Hakomori SI, Childs RA, Feizi T (1979) *J Biol Chem* 254:3221–3228.
5. Clausen H, Hakomori S (1989) *Vox Sang* 56:1–20.
6. Inaba N, Hiruma T, Togayachi A, Iwasaki H, Wang XH, Furukawa Y, Sumi R, Kudo T, Fujimura K, Iwai T, *et al.* (2003) *Blood* 101:2870–2876.
7. Lowe JB, Stoolman LM, Nair RP, Larsen RD, Berhend TL, Marks RM (1990) *Cell* 63:475–484.
8. Fukuda M, Hiraoka N, Yeh JC (1999) *J Cell Biol* 147:467–470.
9. Lowe JB (2001) *Cell* 104:809–812.
10. Comelli EM, Sutton-Smith M, Yan Q, Amado M, Panico M, Gilmartin T, Whisenant T, Lanigan CM, Head SR, Goldberg D, *et al.* (2006) *J Immunol* 177:2431–2440.
11. Gilbert CW, Zaroukian MH, Esselman WJ (1988) *J Immunol* 140:2821–2828.
12. Ohyama C, Tsuboi S, Fukuda M (1999) *EMBO J* 18:1516–1525.
13. Saito H, Nishikawa A, Gu J, Ihara Y, Soejima H, Wada Y, Sekiya C, Niikawa N, Taniguchi N (1994) *Biochem Biophys Res Commun* 198:318–327.
14. Demetriou M, Granovsky M, Quaggin S, Dennis JW (2001) *Nature* 409:733–739.
15. Togayachi A, Sato T, Narimatsu H (2006) *Methods Enzymol* 416:91–102.
16. Shiraishi N, Natsume A, Togayachi A, Endo T, Akashima T, Yamada Y, Imai N, Nakagawa S, Koizumi S, Sekine S, *et al.* (2001) *J Biol Chem* 276:3498–3507.
17. Togayachi A, Akashima T, Ookubo R, Kudo T, Nishihara S, Iwasaki H, Natsume A, Mio H, Inokuchi J, Irimura T, *et al.* (2001) *J Biol Chem* 276:22032–22040.
18. Kawashima H, Sueyoshi S, Li H, Yamamoto K, Osawa T (1990) *Glycoconj J* 7:323–334.
19. Nachbar MS, Oppenheim JD (1982) *Methods Enzymol* 83:363–368.
20. Tsubata T (1999) *Curr Opin Immunol* 11:249–255.
21. Cummings RD, Kornfeld S (1984) *J Biol Chem* 259:6253–6260.
22. Elices MJ, Goldstein IJ (1990) *Carbohydr Res* 203:109–118.
23. Feizi T, Childs RA, Watanabe K, Hakomori SI (1979) *J Exp Med* 149:975–980.
24. Henion TR, Zhou D, Wolfer DP, Jungalwala FB, Hennet T (2001) *J Biol Chem* 276:30261–30269.
25. Ward SG (1996) *Biochem J* 318:361–377.
26. Ma BY, Mikolajczak SA, Yoshida T, Yoshida R, Kelvin DJ, Ochi A (2004) *Biochem Biophys Res Commun* 317:60–67.
27. Buhl AM, Pleiman CM, Rickert RC, Cambier JC (1997) *J Exp Med* 186:1897–1910.
28. Childs RA, Dalchau R, Scudder P, Hounsell EF, Fabre JW, Feizi T (1983) *Biochem Biophys Res Commun* 110:424–431.
29. Childs RA, Feizi T (1981) *Biochem Biophys Res Commun* 102:1158–1164.
30. Sato T, Furukawa K, Autero M, Gahmberg CG, Kobata A (1993) *Biochemistry* 32:12694–12704.
31. Furukawa K, Funakoshi Y, Autero M, Horejsi V, Kobata A, Gahmberg CG (1998) *Eur J Biochem* 251:288–294.
32. Lau KS, Partridge EA, Grigorian A, Silvescu CI, Reinhold VN, Demetriou M, Dennis JW (2007) *Cell* 129:123–134.
33. Rudd PM, Wormald MR, Stanfield RL, Huang M, Mattsson N, Speir JA, DiGennaro JA, Fetrow JS, Dwek RA, Wilson IA (1999) *J Mol Biol* 293:351–366.
34. Lowe JB (2003) *Curr Opin Cell Biol* 15:531–538.
35. Varki A, Angata T (2006) *Glycobiology* 16:1R–27R.
36. Brewer CF, Miceli MC, Baum LG (2002) *Curr Opin Struct Biol* 12:616–623.
37. Hirabayashi J, Hashidate T, Arata Y, Nishi N, Nakamura T, Hirashima M, Urashima T, Oka T, Futai M, Muller WE, *et al.* (2002) *Biochim Biophys Acta* 1572:232–254.
38. Ferrero E, Jiao D, Tsuberi BZ, Tesio L, Rong GW, Haziot A, Goyert SM (1993) *Proc Natl Acad Sci USA* 90:2380–2384.
39. Zambrowicz BP, Friedrich GA, Buxton EC, Lilleberg SL, Person C, Sands AT (1998) *Nature* 392:608–611.
40. Takasaki S, Mizuochi T, Kobata A (1982) *Methods Enzymol* 83:263–268.
41. Yamashita K, Mizuochi T, Kobata A (1982) *Methods Enzymol* 83:105–126.
42. Kuno A, Uchiyama N, Koseki-Kuno S, Ebe Y, Takashima S, Yamada M, Hirabayashi J (2005) *Nat Methods* 2:851–856.
43. Novak EJ, Rabinovitch PS (1994) *Cytometry* 17:135–141.